HOPF BIFURCATION ANALYSIS OF DISTRIBUTED DELAYS EQUATIONS

Franco S. Gentile
Dpto. de Matemática
Universidad Nacional del Sur
Instituto de Investigaciones en Ingeniería Eléctrica (IIIE)
UNS-CONICET
(8000) Bahía Blanca, Argentina
fsgentile@gmail.com

Jorge L. Moiola
Instituto de Investigaciones en Ingeniería Eléctrica (IIIE)
UNS-CONICET
Depto. de Ingeniería Eléctrica y de Computadoras
Universidad Nacional del Sur
(8000) Bahía Blanca, Argentina
jmoiola@criba.edu.ar

Abstract
In this article, we develop a modified version of the graphical Hopf bifurcation theorem for capturing smooth oscillations of delay differential equations with distributed delays. Our approach relies on a simple interpretation of the effect of the distributed delay based on the Laplace transform. The theoretical results are illustrated with an example of neural networks.

Key words
Delay-differential equations, distributed delays, Hopf bifurcation.

1 Introduction

Delay-differential equations (DDEs) often arise when modeling systems in biology, control, physics, and other research areas. Particularly, distributed delays have been widely used in biological issues, for example, in the cellular spread of diseases [Culshaw, Ruan and Webb, 2003], prey-predator systems [Ruan, 2006], epidemic models [Arino and van der Driessche, 2006], etc. In such systems, distributed delay leads to more accurate models than discrete (constant) delays, because the former can describe uncertainties in the delay value, memory effects, modification of the delay due to unmodeled factors, etc.

DDEs with distributed delays are given by integro-differential equations, which are a bit difficult to deal with. In most cases, a set of equations equivalent to the original model is attained. That set may involve ordinary differential equations (ODEs) as well as DDEs with discrete delays. Unfortunately, this procedure depends strongly on the characteristics of the delay distribution (see, for example [Rasmussen, Wake and Donaldson, 2003; Liao, Li and Chen, 2004]).

Among the most sophisticated theoretical results about stability of DDEs with distributed delays are [Anderson, 1992; Bernard, Bélair and Mackey, 2001; Crauste, 2010], but those only refer to scalar equations. Also, the numerical results in [Atay, 2003] give important insights about the effect of the spread of the delay distribution on the dynamics of coupled oscillators.

In this article, we propose a modified version of the method based on the graphical Hopf bifurcation theorem (GHBT for short) [Mees and Chua, 1979; Moiola and Chen, 1996] for analyzing bifurcations in DDEs with distributed delays. Our current approach is a generalization of the results presented in [Gentile, Moiola and Paolini, 2012], in which DDEs with constant delays were considered. In DDEs with distributed delays, the influence of the past history is determined by a function called kernel or distribution. The development of our approach does not depend on the particular shape of that function, and we only require less restrictive conditions from it. Moreover, our setting shows that the effect of the delay distribution can be described simply by using properties of the Laplace transform. We conclude with an example of coupled neurons, for which several bifurcation diagrams are found using the proposed methodology.

2 Preliminaries

In this section we briefly outline the GHBT method for systems described by ODEs. A detailed presentation of this technique can be found in [Mees and Chua, 1979; Moiola and Chen, 1996]. Let us consider the autonomous system

$$\dot{\mathbf{x}}(t) = \mathbf{f}\left[\mathbf{x}(t); \mu\right], \tag{1}$$

where $\mathbf{x}(t) \in \mathbb{R}^n$, $\mu \in \mathbb{R}$ is a parameter, $\mathbf{f} : \mathbb{R}^n \times \mathbb{R} \to \mathbb{R}^n$ is a smooth (at least $\mathcal{C}^4$) nonlinear function and $\dot{\mathbf{x}}(t) \triangleq \frac{d}{dt}\mathbf{x}(t)$. By choosing adequate matrices $A \in \mathbb{R}^{n\times n}$, $B \in \mathbb{R}^{n\times p}$, $C \in \mathbb{R}^{m\times n}$, Eq. (1) can be recast as

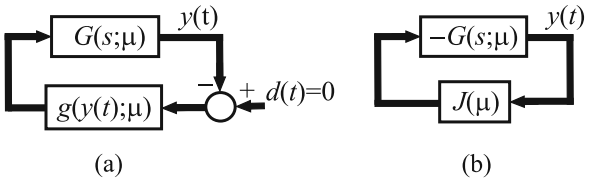

Figure 1. (a): Block representation of system (2); (b): Linearized feedback loop.

$$\begin{cases} \dot{\mathbf{x}}(t) = A\mathbf{x}(t) + B\mathbf{g}\left[\mathbf{y}(t);\mu\right], \\ \mathbf{y}(t) = -C\mathbf{x}(t), \end{cases} \tag{2}$$

where $\mathbf{g} : \mathbb{R}^m \times \mathbb{R} \to \mathbb{R}^p$ and $\mathbf{y}(t)$ is the output of the standard state-space approach. Then, by applying the Laplace transform to the system above (with zero initial condition), we have

$$\begin{aligned} &\mathcal{L}\{\mathbf{x}(t)\} = (sI_n - A)^{-1}B\mathcal{L}\{\mathbf{g}\left[\mathbf{y}(t);\mu\right]\}, \\ &\mathcal{L}\{\mathbf{y}(t)\} = -C\mathcal{L}\{\mathbf{x}(t)\} = -G(s;\mu)\mathcal{L}\{\mathbf{g}\left[\mathbf{y}(t);\mu\right]\}, \end{aligned} \tag{3}$$

where I_n denotes the $n \times n$ identity matrix, $s \in \mathbb{C}$ and $G(s;\mu) \triangleq C(sI_n - A)^{-1}B$ is a transfer function representing the linear part of (2)[1]. System (2) can be represented as shown in Fig. 1(a), in which $\mathbf{d}(t) = 0$ denotes that the system is autonomous. Let us suppose the existence of at least one equilibrium point $\widehat{\mathbf{x}}$ of (1). The corresponding equilibrium $\widehat{\mathbf{y}}$ of the feedback system (2) is given by $\widehat{\mathbf{y}} = -C\widehat{\mathbf{x}}$. By computing the Jacobian matrix

$$J(\mu) = \left.\frac{\partial \mathbf{g}(\mathbf{y};\mu)}{\partial \mathbf{y}}\right|_{\mathbf{y}=\widehat{\mathbf{y}}},$$

we obtain the linearized loop shown in Fig. 1(b). With the aim of detecting bifurcations in the nonlinear system (1), it is useful to consider the following result, developed in [Mees and Chua, 1979].

Lemma 1 If an eigenvalue of the matrix of linearization of system (1) around $\widehat{\mathbf{x}}$, assumes a purely imaginary value $i\omega_0$ at a particular value $\mu = \mu_0$, then an eigenvalue of the constant matrix $G(i\omega_0;\mu_0)J(\mu_0)$ must assume the value $-1 + i0$ at $\mu = \mu_0$. ■

The eigenvalues λ_k, $k = 1, ..., m$ of $G(s;\mu)J(\mu)$ are the roots of the characteristic polynomial

$$\begin{aligned} h(\lambda, s;\mu) &:= \det(\lambda I_m - GJ) \\ &= \lambda^m + a_{m-1}(s;\mu)\lambda^{m-1} + \ldots + a_0(s;\mu), \end{aligned} \tag{4}$$

where $a_j(s;\mu)$, $j = 0, ..., m-1$ are rational functions in the variable s [MacFarlane and Postlethwaite, 1977]. The equation $h(\lambda, s;\mu) = 0$ is called characteristic equation in the frequency domain. Let us suppose that the equilibrium of (2) is stable for $\mu < \mu_0$ and unstable for $\mu > \mu_0$, and that, for $\mu = \mu_0$, there is a simple root $\widehat{\lambda}(s;\mu)$ of $h(\lambda, s;\mu) = 0$ that takes the value $-1 + i0$ for a given $s = i\omega_0$. Hence, $\mu = \mu_0$ is a bifurcation point in the parameter space. If $\omega_0 \neq 0$ ($\omega_0 = 0$) the bifurcation is called *dynamic* or *Hopf* (*static*). Let us focalize on Hopf bifurcations, which are responsible for the appearance of smooth oscillations. If we consider the geometrical locus of $\widehat{\lambda}(i\omega;\mu)$, it can be viewed as a Nyquist curve in the complex plane, parameterized on the variable ω, which describes a different contour for each fixed value of μ. Particularly, by picking $\mu = \mu_0$, this curve crosses the point $-1 + i0$ at $\omega = \omega_0$. Now, let us consider the auxiliary complex number

$$\xi(\omega;\mu) = -\mathbf{w}^T G(i\omega;\mu)\mathbf{p}(\omega;\mu) / \left[\mathbf{w}^T\mathbf{v}\right], \tag{5}$$

where $\mathbf{p}(\cdot)$ is a vectorial quantity depending on the high-order derivatives of $\mathbf{g}\left[\mathbf{y}(t);\mu\right]$ and will be defined later, and $\mathbf{v}, \mathbf{w}$ are the right and left eigenvectors of $G(i\omega;\mu)J(\mu)$ associated to $\widehat{\lambda}(i\omega;\mu)$. Now, let μ vary slightly from μ_0, and consider the following theorem given in [Mees and Chua, 1979; Moiola and Chen, 1996], which is briefly stated as follows:

Theorem 1 (Graphical Hopf Bifurcation Theorem) Suppose that when ω varies, $\xi(\omega;\mu) \neq 0$, and that the half line starting from $-1+i0$ and pointing to the direction of $\xi(\omega;\mu)$ [2], first intersects the locus of $\widehat{\lambda}(i\omega;\mu)$ at the point

$$P = \widehat{\lambda}(i\widetilde{\omega};\mu) = -1 + \xi(\widetilde{\omega};\mu)\theta^2, \tag{6}$$

where $\theta = \theta(\widetilde{\mu}) \geq 0$. Suppose, furthermore, that the above intersection is transversal, *i.e.*, $\widehat{\lambda}(i\widetilde{\omega};\mu)$ and $\xi(\widetilde{\omega};\mu)$ are not parallel. Then:

1. The nonlinear system (1) has an isolated periodic solution centered at $\widehat{\mathbf{x}}$.
2. If the total number of anticlockwise encirclements of the point $P + \delta\xi(\widetilde{\omega};\mu)$, for a small enough δ, is equal to the number of poles of $\widehat{\lambda}(s;\mu)$ with positive real parts, then the limit cycle is stable. ■

It is worth mentioning that θ is a measure of the amplitude and $\widetilde{\omega}$ is the approximate frequency of the periodic solution. If the hypotheses of Theorem 1 are fulfilled, that solution can be described accurately enough by the second-order Fourier expansion

$$\mathbf{y}(t) \simeq \widehat{\mathbf{y}} + \Re\left\{\sum_{k=0}^{2} \mathcal{Y}^k e^{ik\widetilde{\omega}t}\right\}, \tag{7}$$

where coefficients $\mathcal{Y}^k$ are given below and $\Re(\cdot)$ means the real part. Vector $\mathbf{p}(\cdot)$ in (5) represents the component of fundamental frequency of $\mathbf{g}\left[\mathbf{y}(t);\mu\right]$ and is given by

[1] By using the notation $G(s;\mu)$ we emphasize the usual dependence of matrices A, B and C on the parameter μ.

[2] By considering ξ as a vector in the complex plane.

$$\mathbf{p}(\omega_0;\mu) = (\mathbf{D}^2\mathbf{g})\mathbf{v}\otimes\mathbf{v}_{02} + \tfrac{1}{2}(\mathbf{D}^2\mathbf{g})\bar{\mathbf{v}}\otimes\mathbf{v}_{22} + \tfrac{1}{8}(\mathbf{D}^3\mathbf{g})\mathbf{v}\otimes\mathbf{v}\otimes\bar{\mathbf{v}}, \tag{8}$$

where $\otimes$ denotes the tensor product operator and

$$(\mathbf{D}^j\mathbf{g}) \triangleq \left.\frac{\partial \mathbf{g}^j(\mathbf{y};\mu)}{\partial \mathbf{y}^j}\right|_{\mathbf{y}=\hat{\mathbf{y}}} \in \mathbb{R}^{p\times m^j}.$$

Tensors $\mathbf{v}_{02}$ and $\mathbf{v}_{22}$ represent the normalized zero and second harmonic components, respectively, of $\mathbf{y}(t)$ in (7), and are computed as

$$\begin{aligned}\mathbf{v}_{02} &= -\tfrac{1}{4}H(0;\mu)(\mathbf{D}^2\mathbf{g})\mathbf{v}\otimes\bar{\mathbf{v}},\\ \mathbf{v}_{22} &= -\tfrac{1}{4}H(i2\omega;\mu)(\mathbf{D}^2\mathbf{g})\mathbf{v}\otimes\mathbf{v}.\end{aligned} \tag{9}$$

where $H(s;\mu) \triangleq (I + G(s;\mu)J(\mu))^{-1}G(s;\mu)$ is called the closed-loop transfer function. By using (9) together with $\theta(\mu)$ and $\widetilde{\omega}(\mu)$ obtained from (6), we find the $\mathcal{Y}^k$ coefficients in (7) as

$$\mathcal{Y}^0 = \theta(\mu)^2\mathbf{v}_{02}, \quad \mathcal{Y}^1 = \theta(\mu)\mathbf{v}, \quad \mathcal{Y}_2 = \theta(\mu)^2\mathbf{v}_{22}, \tag{10}$$

and finally we approximate the periodic solution from (7). Also, the stability of this periodic orbit can be determined algebraically via the *curvature coefficient*, which is given by

$$\sigma_0 = \Re\left\{\xi(\omega_0;\mu)\mathbf{w}^T\mathbf{v}/\left[\mathbf{w}^T G'(i\omega_0;\mu)J(\mu)\mathbf{v}\right]\right\}, \tag{11}$$

where $G'(i\omega;\mu) := \partial G(s;\mu)/\partial s|_{s=i\omega}$. Then, if σ_0 is *negative* (*positive*), the Hopf bifurcation is *supercritical* (*subcritical*); if $\hat{\mathbf{y}}$ loses its stability at bifurcation, then a *stable* (*unstable*) periodic solution exists when the equilibrium is *unstable* (*stable*).

3 Alternative formulation for DDEs with distributed delays

The general form of a DDE with distributed delay can be stated as follows

$$\dot{\mathbf{x}}(t) = \mathbf{f}\left[\mathbf{x}(t), \int_{-\infty}^{t}\mathbf{x}(u)k(t-u)du;\mu\right], \tag{12}$$

where $\mathbf{x}\in\mathbb{R}^n$, $\mu\in\mathbb{R}$ is the bifurcation parameter, $\mathbf{f}:\mathbb{R}^n\times\mathbb{R}^n\times\mathbb{R}\to\mathbb{R}^n$ in a smooth nonlinear functional and $k(\cdot)$ is the (scalar) kernel function. Equations as (12) have been studied by many authors, mostly in biological applications (see, for example [Culshaw, Ruan and Webb, 2003; Ruan, 2006]). In order to deal with integro-differential equations like (12), the most common approach is to find an equivalent system, given by a set of ODEs o DDEs (avoiding the explicitness of integral terms). But this trick has an important disadvantage: the number of additional equations that must be introduced and their kind (ODEs or DDEs) depend strongly on the particular shape of the kernel (see, for example [Culshaw, Ruan and Webb, 2003; Rasmussen, Wake and Donaldson, 2003; Liao, Li and Chen, 2004]).

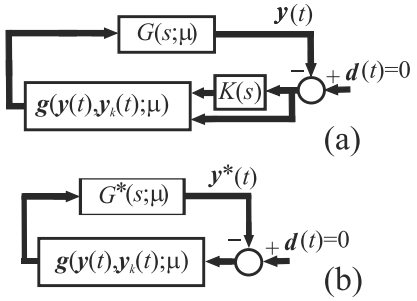

Figure 2. (a) Block representation of system (13). (b) Equivalent system with the extended matrix $G^*(s;\mu)$.

In this work, we propose a modified version of the algorithm given in Section 1 for studying Hopf bifurcations in equations like (12). Choosing adequate matrices $A\in\mathbb{R}^{n\times n}$, $B\in\mathbb{R}^{n\times p}$ and $C\in\mathbb{R}^{m\times n}$, Eq. (12) can be recast as the feedback system

$$\begin{cases}\dot{\mathbf{x}}(t) = A\mathbf{x}(t) + B\mathbf{g}\left[\mathbf{y}(t),\mathbf{y}_k(t);\mu\right],\\ \mathbf{y}(t) = -C\mathbf{x}(t),\end{cases} \tag{13}$$

where $\mathbf{y}_k(t) \triangleq \int_{-\infty}^{t}\mathbf{y}(u)k(t-u)du$. Thus, by applying the Laplace transform as in (3), we have

$$\begin{aligned}\mathcal{L}\{\mathbf{x}(t)\} &= (sI_n - A)^{-1}B\mathcal{L}\{\mathbf{g}\left[\mathbf{y}(t),\mathbf{y}_k(t);\mu\right]\},\\ \mathcal{L}\{\mathbf{y}(t)\} &= -G(s;\mu)\mathcal{L}\{\mathbf{g}\left[\mathbf{y}(t),\mathbf{y}_k(t);\mu\right]\},\end{aligned} \tag{14}$$

where $G(s;\mu) = C(sI_n - A)^{-1}B$. From the convolution property, for the "retarded" quantities, we have

$$\begin{aligned}\mathcal{L}\{\mathbf{x}_k(t)\} &= \mathcal{L}\{\mathbf{x}(t)\}K(s),\\ \mathcal{L}\{\mathbf{y}_k(t)\} &= -C\mathcal{L}\{\mathbf{x}_k(t)\} = -C\mathcal{L}\{\mathbf{x}(t)\}K(s)\end{aligned} \tag{15}$$

where $K(s) \triangleq \mathcal{L}\{k(t)\}$. System (13) is represented in Fig. 2(a). Notice that both $\mathbf{y}(t)$ and $\mathbf{y}_k(t)$ act as inputs of the nonlinear block $\mathbf{g}[\,\cdot\,]$. In order to apply the GHBT, we would like to find an equivalent block representation consisting of a single linear system with a nonlinear feedback as the configuration shown in Fig. 1(a). This objective can be achieved by defining an extended matrix

$$G^*(s;\mu) \triangleq \begin{pmatrix}G(s;\mu)\\ G(s;\mu)K(s)\end{pmatrix} \in \mathbb{R}^{2m\times p}, \tag{16}$$

thus absorbing the delay block into the forward path as shown in Fig. 2(b), where $\mathbf{y}^*(t)$ denotes the "extended" output

$$\mathbf{y}^*(t) \triangleq \begin{pmatrix}\mathbf{y}(t)\\ \mathbf{y}_k(t)\end{pmatrix} \in \mathbb{R}^{2m}. \tag{17}$$

Moreover, the methodology of Section 1 can be applied without further modifications. When linearizing, the Jacobian matrix must be computed as

$$J^*(\mu) = \left(\frac{\partial \mathbf{g}(\mathbf{y},\mathbf{y}_k;\mu)}{\partial \mathbf{y}} \;\middle|\; \frac{\partial \mathbf{g}(\mathbf{y},\mathbf{y}_k;\mu)}{\partial \mathbf{y}_k} \right) \Big|_{\mathbf{y}^*=\widehat{\mathbf{y}}^*} \quad (18)$$

All the formulae presented in Section 1 remain valid, with the obvious dimensional augmentation of matrices and vectors. The rigorous proof of this assertion is a little more involved than the one given in [Gentile, Moiola and Paolini, 2012] for systems with *constant* delays, but it is quite long to be included here. The constant delay is obtained by taking $k(t) = \delta(t-\tau)$ in (12), where $\tau > 0$ is constant and δ is the Dirac delta distribution. So, the present results are more general than the ones presented in the cited text.

4 Example: Neurons with delayed coupling

The following model has been studied in [Liao, Wong and Wu, 2001] and it represents a two-neuron system with distribute delays

$$\begin{cases} \dot{x}_1(t) = -x_1(t) + a_1 f\left[x_2(t) - b_2 x_{2k}(t)\right], \\ \dot{x}_1(t) = -x_2(t) + a_2 f\left[x_1(t) - b_1 x_{1k}(t)\right], \\ x_{ik}(t) \triangleq \int_{-\infty}^{t} k(t-u) x_i(u) du, \; i = 1, 2, \end{cases} \quad (19)$$

where $a_i, b_i \geq 0$. Here, $x_i(t)$ represent the mean soma potential of the neuron, a_i denotes the range of the variables x_i, and b_i are measures of the inhibitory influence of the past history. We assume that $f(\cdot)$ is smooth and verifies $f(0) = 0, \quad f'(0) \triangleq f' > 0$. For the kernel, we consider a gamma distribution

$$k_a^p(u) = \frac{a^p u^{p-1} e^{-au}}{(p-1)!}, \; u \geq 0. \quad (20)$$

In [Liao, Wong and Wu, 2001], the authors used the so-called weak kernel, obtained from (20) with $p = 1$. They studied the Hopf bifurcations arising in Eq. (19) through the normal form theory.

Here, we begin our analysis without picking a particular value of p. In order to apply the formulation given in Section 2, we choose

$$A = \begin{pmatrix} -1 & 0 \\ 0 & -1 \end{pmatrix}, \quad B = C = I_2,$$
$$\mathbf{g}\left[\mathbf{y}^*(t);\mu\right] = \begin{pmatrix} a_1 f(b_2\, y_{2k} - y_2) \\ a_2 f(b_1\, y_{1k} - y_1) \end{pmatrix},$$

where $y_{ik}(t) := -x_{ik}(t)$ and now μ denotes the set of parameters. For the linear part (see Fig. 2(a)) we have

$$G^*(s) = \begin{pmatrix} G(s) \\ G(s)K(s) \end{pmatrix}, \quad G(s) = \frac{1}{s+1} I_2.$$

As $f(0) = 0$, it follows that $(\widehat{x}_1, \widehat{x}_2) = (0,0)$ is an equilibrium point of (19), then $\widehat{\mathbf{y}}^* = 0$. From (18), we have

$$J^*(\mu) = f' \begin{pmatrix} 0 & -a_1 & 0 & a_1 b_2 \\ -a_2 & 0 & a_2 b_1 & 0 \end{pmatrix},$$

The characteristic equation $h(\lambda, s; \mu) = |\lambda I_4 - G^*(s) J(\mu)| = 0$ results

$$h(\lambda, s; \mu) = \tfrac{\lambda^2}{(s+1)^2} \left\{ \lambda^2 (s+1)^2 - a_1 a_2 (f')^2 \left[b_1 K(s) - 1\right] \left[b_2 K(s) - 1\right] \right\} = 0. \quad (21)$$

The case $b_1 = b_2$ is clearly simpler than the general case $b_1 \neq b_2$. Then, we shall study the former first.

4.1 Symmetrical case ($b_1 = b_2$)

In this case, we suppose that the past influence is identical for the two neurons ($b_1 = b_2 = b$). From (21), it is obtained

$$\widehat{\lambda}(s;\mu) = \delta \frac{[bK(s) - 1]}{s+1},$$

where $\delta \triangleq \sqrt{a_1 a_2} f'$. For the gamma kernel (20), we have $K_a^p(s) = a^p/(s+a)^p$ and the Hopf bifurcation condition $\widehat{\lambda}(i\omega_0;\mu) = -1$ becomes

$$a^p b \delta = (\delta - 1 - i\omega_0)(a + i\omega_0)^p. \quad (22)$$

Also, picking $\omega_0 = 0$ we find the existence of a static bifurcation for $\delta = \delta_{ST} := 1/(1-b)$.

Weak kernel **($p = 1$)**

For the so-called *weak* kernel, Eq. (22) becomes

$$ab\delta = a(\delta - 1) + \omega_0^2 + i\omega_0(\delta - 1 - a),$$

which yields the solution

$$a = \delta - 1, \quad \omega_0 = \sqrt{(\delta - 1)[\delta(b-1) + 1]}.$$

As $\omega_0 \in \mathbb{R}$, the conditions $\delta > 1$ and $\delta(b-1) + 1 > 0$ must be fulfilled. In the limit case $\delta = \delta_{ST} = 1/(1-b)$, the critical frequency approaches zero, and the Hopf bifurcation curve collides with a static (ST) bifurcation at a Bogdanov-Takens (BT) point. Figure 3 shows the bifurcation diagram for $b = 1/2$. In the Hopf curves, H$-$ indicates that the curvature coefficient computed from (11) is negative along them. This means that a stable limit cycle emerges when the equilibrium point switches from stable to unstable.

Strong kernel **($p = 2$)**

In this case, Eq. (22) results

$$a^2 b\delta = (\delta - 1)(a^2 - \omega_0^2) + 2a\omega_0^2 + i\omega_0[2a(\delta - 1) + \omega_0^2 - a^2].$$

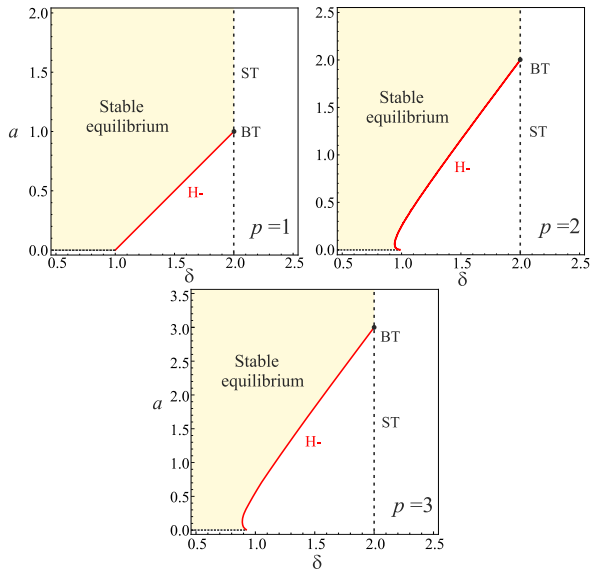

Figure 3. Bifurcation diagrams for system (19) with a gamma kernel and different values of p, with $b_1 = b_2 = 1/2$.

Splitting into real and imaginary parts, and then solving, it is obtained

$$\begin{aligned} \omega_0^2 &= a^2 - 2a(\delta - 1), \\ ab\delta &= 2(\delta - 1 - a)^2. \end{aligned} \tag{23}$$

The equation above defines implicitly the Hopf curve in the (δ, a) parameter space (for fixed values of b). As before, as the critical frequency ω_0 tends to zero, the Hopf curve approaches the BT point for $\delta_{ST} = 1/(1-b)$. Figure 3 shows the bifurcation diagram, where again we considered $b = 1/2$.

Gamma kernel with $p = 3$

By taking $p = 3$ in (22), we obtain

$$b\delta a^3 = (\delta - 1 - i\omega_0)\left[a(a^2 - 3\omega_0^2) + i\omega_0(3a^2 - \omega_0^2)\right],$$

which can be solved yielding

$$\begin{aligned} \omega_0^2 &= a^2[3(\delta - 1) - a]/\left[\delta - 1 - 3a\right], \\ \omega_0^4 &+ 3a(\delta - a - 1)\omega_0^2 + a^3[\delta(b-1) - 1] = 0. \end{aligned} \tag{24}$$

Replacing the expression of ω_0 into the second equation, the Hopf bifurcation condition can be stated as $F(\delta, a) = 0$, where $F(\delta, a)$ is a polynomial in δ and a (again, taking fixed values of b). Thus, $F(\delta, a) = 0$ defines implicitly the Hopf curve in the (δ, a) space, as shown in Fig. 3 for $p = 3$.

4.2 General case ($b_1 \neq b_2$)

In the asymmetrical case, from (21) we obtain

$$\widehat{\lambda}^2 = \frac{\delta^2 \left[b_1 K(s) - 1\right]\left[b_2 K(s) - 1\right]}{(s+1)^2}, \tag{25}$$

where $\delta = \sqrt{a_1 a_2} f'$ as before. For a complex number w, let us consider the branch of the square root such that $\sqrt{w} = \sqrt{|w|} e^{i\theta/2}$, where $\theta := \mathrm{Arg}\{w\}$, $0 \leq \mathrm{Arg}\{w\} < 2\pi$. Then, $\widehat{\lambda}(s;\mu)$ is expressed as

$$\widehat{\lambda}(s;\mu) = \frac{\delta \sqrt{b_1 K(s) - 1}\sqrt{b_2 K(s) - 1}}{s+1}. \tag{26}$$

The equation above allows studying not only asymmetries in coefficients b_i but also asymmetries in the two kernels. For $s = 0$ in (26), we obtain the condition for a static bifurcation as $\delta_{ST} = \frac{1}{\sqrt{(b_1-1)(b_2-1)}}$. From (25), the Hopf bifurcation condition can be expressed as

$$(1 + i\omega_0)^2 - \delta^2 \left[b_1 K(i\omega_0) - 1\right]\left[b_2 K(i\omega_0) - 1\right] = 0,$$

which for the *gamma kernel* $K_a^p(s) = a^p/(s+a)^p$, becomes

$$\begin{aligned} (1 + i\omega_0)^2 (a + i\omega_0)^{2p} - \delta^2 \left[b_1 a^p - (a + i\omega_0)^p\right] \\ \times \left[b_2 a^p - (a + i\omega_0)^p\right] = 0. \end{aligned} \tag{27}$$

For example, for the *weak* kernel, we have

$$(1 + i\omega_0)^2 (a + i\omega_0)^2 - \delta^2 \left[a b_1^* - i\omega_0\right]\left[a b_2^* - i\omega_0\right] = 0,$$

where $b_1^* \triangleq b_1 - 1$ and $b_2^* \triangleq b_2 - 1$. Splitting into real and imaginary parts as before, it is obtained

$$\begin{cases} (a^2 - \omega_0^2)(1 - \omega_0^2) - 4a\omega_0^2 - \delta^2(a^2 b_1^* b_2^* - \omega_0^2) = 0 \\ 2\left[a^2 - \omega_0^2 + a(1 - \omega_0^2)\right] + a\delta^2(b_1^* + b_2^*) = 0. \end{cases} \tag{28}$$

From the second equation we have $\omega_0^2 = a\left[1 + \delta^2(b_1^* + b_2^*)/\left[2(a+1)\right]\right]$, and replacing into the first one, we obtain the condition $F(\delta, a, b_1^*, b_2^*) = 0$, where $F(\cdot)$ is again a polynomial. For example, taking fixed values of b_1^* and b_2^*, we can find the Hopf curve in the (δ, a) space by solving $F(\delta, a) = 0$. Figure 4 shows several bifurcation diagrams obtained with $b_2 = 1/2$ and different values of b_1. As in the symmetrical case, all points along the Hopf curves represent supercritical bifurcations ($\sigma_0 < 0$). Figure 5 shows two Nyquist diagrams and the corresponding ξ vectors for a stable (up) and unstable (down) equilibrium. When the equilibrium is unstable, the intersection between $\widehat{\lambda}$ and ξ predicts the existence of a stable limit cycle, which is confirmed via numerical simulation. In this example, we chose $f(u) = \tanh(u)$ in (19). For this nonlinearity, the auxiliary complex number computed from (5) results

$$\xi(i\omega;\mu) = \frac{a_1|\eta_1|\sqrt{\eta_1\eta_2}(a_1|\eta_1| - a_2|\eta_2|)}{8|K(i\omega)|^2\sqrt{a_1 a_2}(1 + i\omega)}, \tag{29}$$

where $\eta_j \triangleq b_j K(i\omega) - 1$, $j = 1, 2$.

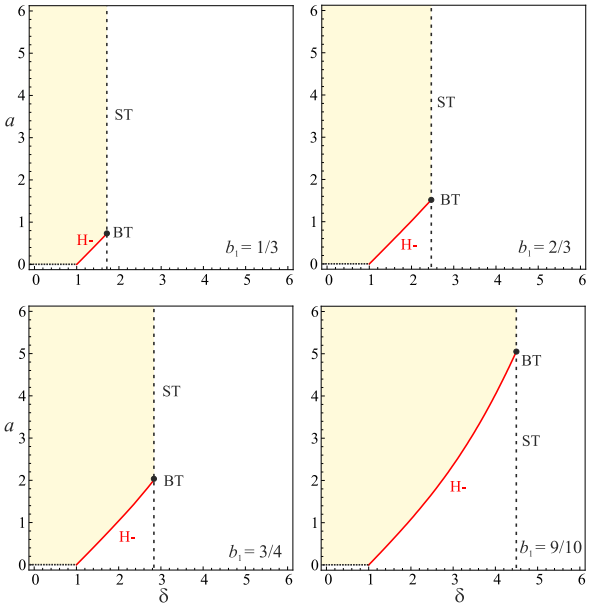

Figure 4. Bifurcation diagrams for system (19) with weak gamma kernel for $b_2 = 1/2$ and different values of b_1. The shaded region represents a stable equilibrium point.

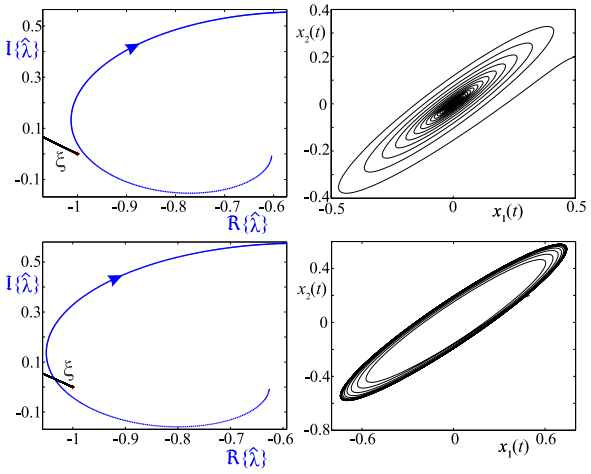

Figure 5. Nyquist diagrams and numerical simulations for system (19) with weak gamma kernel, with $a = 2$, $b_1 = 9/10$, $b_2 = 1/2$ and $a_1 = a_2 = 2.7$ (up, stable equilibrium), $a_1 = a_2 = 2.8$ (down, unstable equilibrium).

5 Conclusion

In this work, we presented a new version of the GHBT which allows the bifurcation analysis of DDEs with distributed delays. This approach provides a simple interpretation of the effect of the distributed delay by taking advantage of the Laplace transform properties. The theoretical results were illustrated through an example of neural networks, for which we have obtained several bifurcation diagrams for gamma kernels.

6 Acknowledgment

The authors thank the financial support of the following grants: PICT 2010-0465 (ANPCyP), PIP 112-200801-01112 (CONICET) and PGI 24/K052 (UNS).

References

Anderson, R. (1992) Intrinsic parameters of differential-delay equations. *J. of Math. Analysis and Applications*, **163**, pp. 184–199.

Arino, J. and van der Driessche P. (2006). *Time delays in epidemic models: Modelling and numerical considerations*. In Arino *et al.* (eds.), Delay Differential Equations and Applications. Springer.

Atay, F. M. (2003) Distributed delays facilitate amplitude death of coupled oscillators. *Physical Review Letters*, **91**(9), pp. 094101(1-4).

Bernard, S., Bélair J. and Mackey M. C. (2001) Sufficient conditions for stability of linear differential equations with distributed delay. *Disc. Cont. Dyn. Syst. Series B*, **1**(2), pp. 233–256.

Crauste, F. (2010). *Stability and Hopf Bifurcation for a First-Order Delay Differential Equation with Distributed Delay*. In Atay (ed.), Complex Time-Delay Systems. Springer.

Culshaw, R. V., Ruan S. and Webb G. (2003) A mathematical model of cell-to-cell spread of HIV-1 that includes a time delay. *J. of Mathematical Biology*, **46**, pp. 425–444.

Gentile, F. S., Moiola J. L. and Paolini E. E. (2012) On the study of bifurcations in delay-differential equations: A frequency-domain approach. *Int. J. of Bifurcation and Chaos*, **22**(6), pp. 1250137(1-15).

Liao, X., Wong K. W. and Wu Z. (2001) Bifurcation analysis on a two-neuron system with distributed delays. *Physica D*, **149**, pp. 123–141.

Liao, X., Li S. and Chen G. R. (2004) Bifurcation analysis on a two-neuron system with distributed delays in the frequency-domain. *Neural Networks*, **17**, pp. 545–561.

MacFarlane A. G. J. & Postlethwaite I. (1977) The generalized Nyquist stability criterion and multivariable root loci, *Int. J. of Control* **25**, pp. 81–127.

Mees, A. I., and Chua L. O. (1979) The Hopf bifurcation theorem and its applications to nonlinear oscillations in circuits and systems. *IEEE Transactions on Circuits and Systems*, **26**(4), pp. 235–254.

Moiola, J. L. and Chen G. R. (1996). *Hopf Bifurcation Analysis: A Frequency Domain Approach*. World Scientific Publishing Co. Singapore.

Rasmussen, H., Wake G. C. and Donaldson J. (2003) Analysis of a class of distributed delay logistic differential equation. *Mathematical and Computer Modelling*, **38**, pp. 123–132.

Ruan, S. (2006). *Delay Differential Equations in Single Species Dynamics*. In NATO Science Series II: Mathematics, Physics and Chemistry. Springer. Berlin.